SAND2024-11132C

GRC Transactions, Vol. 48, 2024

Chloride-based Wireline Tool for Measuring Fracture Inflow in Enhanced Geothermal Systems (EGS) Wells: Field Deployment Updates

Melanie B. Schneider[1], Sarah Sausan[2], Marshall Hartung[2], Roland Horne[2], Alfred H. Cochrane[1], Jiann-cherng Su[1], Andrew A. Wright[1], Taylor Myers[1], Joseph Pope[1], Joshua Tafoya[1]

[1]Sandia National Laboratories

[2]Stanford University

Keywords
Chloride concentration, Fracture Inflows, Utah FORGE, EGS, Chloride, Single-Phase

ABSTRACT

This paper presents the ongoing development of a chloride-based wireline tool designed to detect and quantify inflows from feed zones in geothermal wells. The tool aims to characterize stimulation events in EGS wells at Utah FORGE (Frontier Observatory for Research in Geothermal Energy) and other EGS sites. Successful development of the chloride tool would greatly improve production monitoring of the fractures and enable proactive prescription of additional stimulations over the life of the field, thus helping to improve EGS commercial feasibility.

The recent developments of the chloride tool have focused on preparing for and conducting the field deployment at the Utah FORGE site. The field-scale tool assembly features a FORGE sensor package housing the Ion Selective Electrode (ISE), a pH electrode, and a reference electrode, as well as a Mitco PTS sensor package for secondary downhole measurements. A high-temperature logging tool has been developed and tested to capture and transmit data from the chemical sensors to the surface through a 7-conductor wireline cable. Alongside the development of the field-scale tool, flow experiments were carried out in the artificial well system at the Stanford Geothermal Lab. These experiments provided crucial insights into how the chemical tool responds to different variables, including the chloride concentration in the feed zone, its vertical positioning relative to the feed zone, and the presence of other chemical species in the feed zone fluid. The results highlight the tool's sensitivity to various parameters, underscoring the potential of using chloride concentration measurements as a method for inferring feed zone inflow rates in geothermal wells. The tool was successfully deployed at the Utah FORGE site using a wireline truck in the vertical well 58-32 and the directional production well 16B(78)-32.

1. Introduction

Enhanced Geothermal Systems (EGS) use artificial fractures to increase fluid extraction in less permeable geothermal reservoirs (Huenges, 2016). Artificial fractures are created through hydraulic stimulation and may close over time, reducing the productivity of the EGS wells (Fei et al., 2023). By monitoring the productivity of artificial fractures, operators can prescribe mitigation techniques such as restimulation. Timely interventions can help to keep the fractures open and flowing throughout the geothermal plant's lifetime, which typically lasts between 30 and 50 years (Sullivan et al., 2010).

The pressure-temperature-spinner (PTS) tool is commonly used to measure inflow rates from feed zones, with the spinner part determining the flow rate (Sisler et al., 2015). PTS tools show limitations in wells with low fluid velocity, low enthalpy, and large diameters (Acuña and Arcedera, 2005). The study found that there was an overestimation of the inflow rate in the vertical section compared to the nonvertical section of the well. Furthermore, changes in hole diameter outside of slotted liners will influence spinner rotation, which could be misinterpreted as an actual change in flow rate.

A geochemistry-based alternative to the PTS tool has been developed by Sandia National Laboratory and the Stanford Geothermal Program as part of the Utah Frontier Observatory for Research in Geothermal Energy (FORGE) project. This tool uses an ion-selective electrode to measure chloride concentration in the well fluid via electrical voltage between a sensor formed from a combination of pressed AgS and AgCl powder and a reference electrode formed from pressed AgCl powder (Hess et al., 2014). Chloride concentration readings around the feed zone can be used to calculate the feed zone inflow rate. In this paper, this tool is referred to as the "chloride tool", the tool assembly is shown in Figure 1-1. A major advantage of the chloride tool is that it does not require knowledge of the hole diameter, which is a limitation of PTS tools.

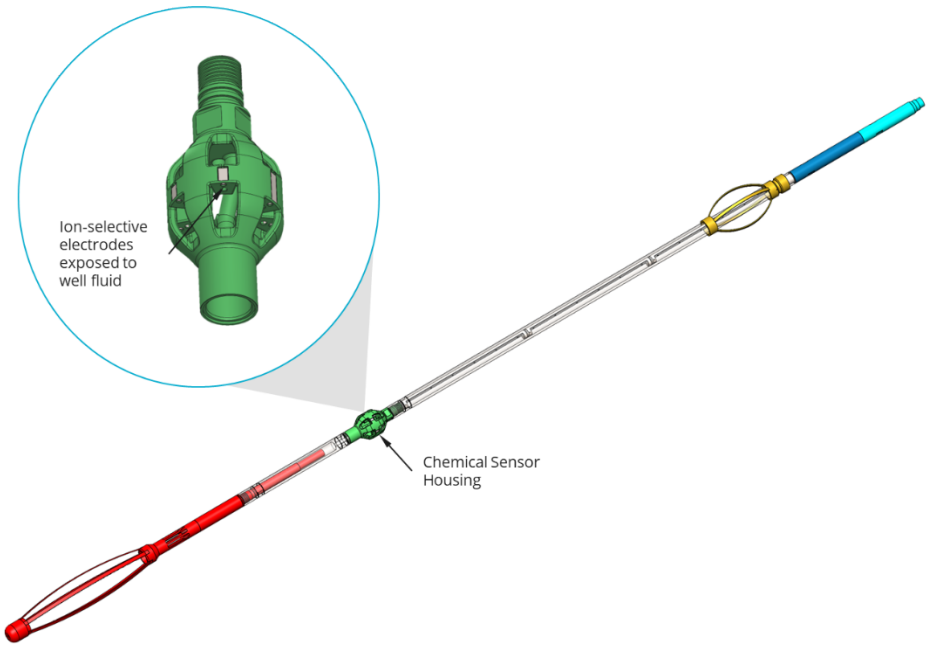

Figure 1-1: Field-deployable chloride tool assembly with close up of chemical sensor housing.

This study expanded on a previous investigation by Gao et al. (2017), which used a similar chloride tool prototype developed by Sandia National Laboratory (Cieslewski et al., 2016; Corbin et al., 2017). In the preliminary study, the team used measurements from the ion-selective electrode to estimate the enthalpy of the feed zone. They targeted chloride concentrations because chloride is consistently present in the liquid phase of geothermal reservoirs. (Sausan, 2023). Building upon that previous research, the current study aimed to develop a field-deployable version of the chloride tool to be used at the Utah FORGE project, which features EGS wells with single-phase fluid and multiple feed zones. This study focused on estimating the feed zone inflow rate, specifically in single-phase flow conditions, rather than enthalpy. The ultimate goal is to leverage insights from the Utah FORGE field trial for broader applications across various EGS sites. More importantly, this study explored a wider role of geochemistry, indicated by the chloride species concentration change, in determining fluid flow patterns in geothermal wells. Typically, the practical application of geochemistry in the geothermal industry revolves around estimating enthalpy or using tracer studies. However, this wider use of geochemistry could enhance our comprehension of the behavior of geothermal wells and fields.

This study employed a multifaceted approach, integrating analytical methods, numerical simulations, laboratory experiments, data science techniques, and field trials. Previously reported progress can be found at Sausan et al. (2021**,** 2023) and Judawisastra et al. (2022, 2023). This paper highlights the latest progress involving field-scale tool fabrication and testing, laboratory setup improvements, and numerical simulations involving the field-scale tool housing and at Utah FORGE temperature and pressure operating conditions. Finally, the successful deployment of the tool at the Utah FORGE site is described.

2. Tool Development and Assembly

2.1 Chloride Tool Assembly

The field-deployable chemical tool assembly incorporates the Mitco PTS sensor package and a tip centralizer at the leading edge of the tool. This is used for secondary downhole measurements to compare the geochemistry-based alternative method to the commonly used PTS measurements. A wire guide component was developed to adapt the PTS tool to the FORGE chemical sensor housing. The sensor wires from both the Mitco PTS tool and the chemical sensors pass through a wire feedthrough in the chemical sensor housing to the high-temperature logging tool in the electronics housing. The electronics housing connects to the wireline via a 4-conductor feedthrough that is adapted to a 7-pin conductor feedthrough that matches the wireline connection. The full assembly schematic is shown in Figure 2-1.

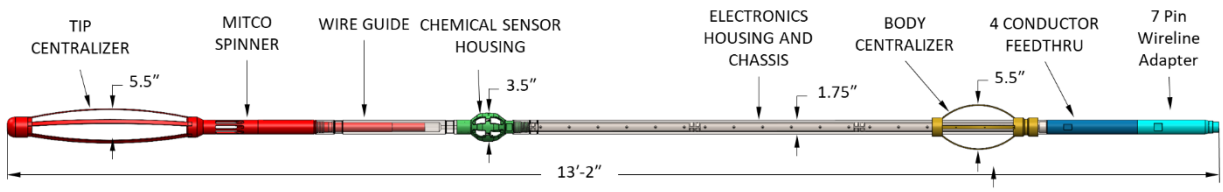

Figure 2-1: Field-deployable chloride tool schematics, including an existing PTS tool adapted to the chloride-based wireline tool and high-temperature developed by Sandia National Laboratory.

2.2 Chemical Sensor Fabrication and Testing

The chloride tool developed by Sandia National Laboratory consists of an ion-specific electrode coupled with a reference electrode. The constituent materials used to develop the ion-selective electrode and reference depend on the ion of interest. The ion-specific electrode probe generates a voltage proportional to the chloride concentration in the fluid, while the reference electrode provides the reference potential for the pair.

The Ion-Specific Electrodes (ISE) probe consists of a pellet formed from an equal part by a mass mixture of Silver Sulfide powder and Silver Chloride (AgS/AgCl) powder. The powder is weighed and transferred to a ¼" diameter die press and compressed to 4000 lbs. and held at constant pressure for 15 minutes. The pellet is then transferred to a preheated oven at 200°C for one hour and then cooled to room temperature.

A CuAg plated pellet wire adapter was fabricated to centralize a high-temperature nickel-plated copper wire on a conductive surface. The CuAg plated pellet wire adapter was attached to the pellets using a high temperature conductive epoxy and cured in a mold to keep the wire adapter centralized on the pellet. The assembled pellets and wire adapters are shown in Figure 2-2. The assembled sensors were then coated with Gagekote #1, a protective coating rated up to 455°C. This configuration of sensor design can then be sealed in the tool assembly using a commercial compression seal feedthrough bulkhead (rated up to 870°C and 10ksi) and allow for multiple sensors to be tested in the same tool.

Figure 2-2: ISE and reference sensor assemblies before application of Gagekote.

To demonstrate the ruggedness of the chemical sensors under High-Pressure, High-Temperature (HPHT) conditions, a laboratory test was conducted using the Sandia autoclave. The sensors and

bulkhead connection design were submerged in 225°C brine at 5000 psi for 24 hours and showed stable measurements. This provided confidence that the chemical sensor design could survive at the Utah FORGE conditions.

To demonstrate the capability of the sensor performance in the chemical composition of the brine at Utah FORGE, samples of flowback water from Utah FORGE Well 16A (78)-32 and 16B(78)-32 were collected and tested using the ISE electrode sensors. The chemical composition of the samples is shown in Table 2-1. Figure 2-3 shows the calibration fit of the well samples in comparison to various molarities of Potassium Chloride (KCl) in distilled water. The voltage measurements of the samples from the flowback in both wells are in good agreement with the measurements of the KCl solution, with lower correlation to the fit line at the lowest chloride concentrations.

Table 2-1: Chemical composition of well samples from Utah FORGE Wells 16A(78)-32 and 16B(78)-32

DATE TIME	LOCATION	Major (mg/l)									
		pH	Na	K	Ca	Mg	B	SiO_2	Cl	SO_4	HCO_3
7/19/2023 20:00	16A(78)-32 Utah FORGE	7.43	621	80.2	92.3	4.13	2.07	167	1300	162	105
7/20/2023 7:50	16B(78)-32 Utah FORGE	6.69	2871	319	44	0.07	9.05	81	4384	239	383
7/20/2023 15:00	16B(78)-32 Utah FORGE	6.64	81	7	109	3.48	0.32	78	122	115	276

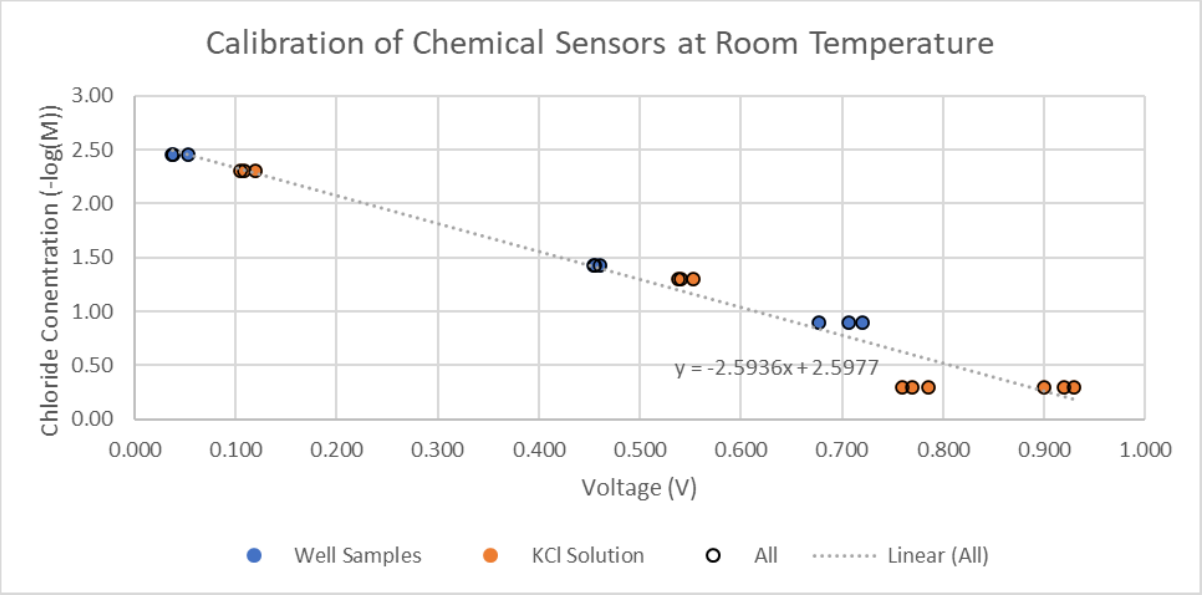

Figure 2-3: Calibration of chloride sensors in KCl solution and samples from wells 16A and 16B for sensors deployed in Utah FORGE Well 16B.

2.2.2 Chemical Sensor Housing

The chemical sensor housing has been designed and developed to enclose the ion-selective chemical sensors, pH Sensor, and the reference electrode sensor. The sensor housing was designed to allow flow to pass through the housing and interact with the chemical sensors uniformly. The housing includes retainer slots to incorporate three Ion-Selective Electrode (ISE) sensors, one reference electrode sensor, and two pH sensors. The sensors are routed through a wire feed-through and sealed using a Conax Compression Seal Fitting. In the current setup, the Conax Compression Seal Fitting can hold up to four wires, this allows for two ISE sensors, one pH sensor, and one reference electrode, the remaining retainer slots are left empty. The housing also includes a wire feed-thru to accommodate the downstream Mitco PTS sensor used for secondary measurements. The unique feature combinations (internal tube, pellet slots) are enabled through metal additive manufacturing. Three sensor housings were manufacture and tested to ensure they are pressure safe and leak resistant. A sensor housing with installed sensors is shown in Figure 2-4.

Figure 2-4: Fabricated sensor housing populated with installed sensors and bulkhead fitting.

2.3 High Temperature Logging Tool

Two versions of the High-Temperature (HT) Logging Tool have been developed and assembled to capture and transmit data from the chloride sensors and PTS spinner tool through the wireline to the surface. The primary version incorporates a modified and previously deployed and tested HT electronics package. The system is composed of three main boards: 1) a digital board featuring a Honeywell HT HT83C51 microcontroller, a Sandia custom high-temperature Application-specific Integrated Circuit (ASIC), and memory, 2) an analog board equipped with an analog to digital converter (ADC), multiplexer, and operation amplifies for the pressure and temperature inputs, and 3) a buffer board that includes a Chemical Buffer Amplifier (CBA) designed to convert the chemical sensor's high input impedance to low impedance. Two full assemblies of the primary HT logging tools have been assembled and tested to confirm operation (see Figure 2-5). The secondary logging tool was constructed to serve as a backup for contingency in the field. This electronic system uses the EV-HT-200CDAQ1 High-Temperature Data Acquisition Reference Design Platform from Analog Devices Inc as an alternative to the digital and analog board in the first system. All three logging tools have been tested to confirm they can accurately capture readings from the chloride and pH sensors, record measurements from the Mitco PTS module, and relay the information through the wireline cable.

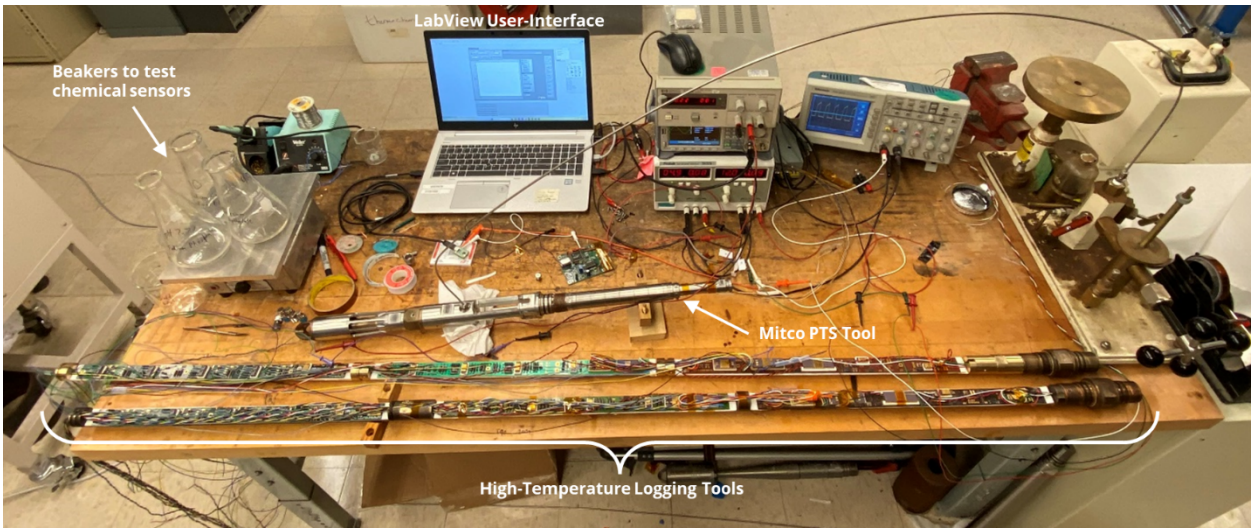

Figure 2-5: Primary High-Temperature Logging Tools being tested to confirm operation in benchtop test.

A LabView user interface has been developed (shown in Figure 2-6) to efficiently handle serial data from the tool, offering real-time data display and recording capabilities on a PC. The interface is designed for compatibility with both the primary and secondary High-Temperature Logging tools. This streamlined field operations for each tool configuration.

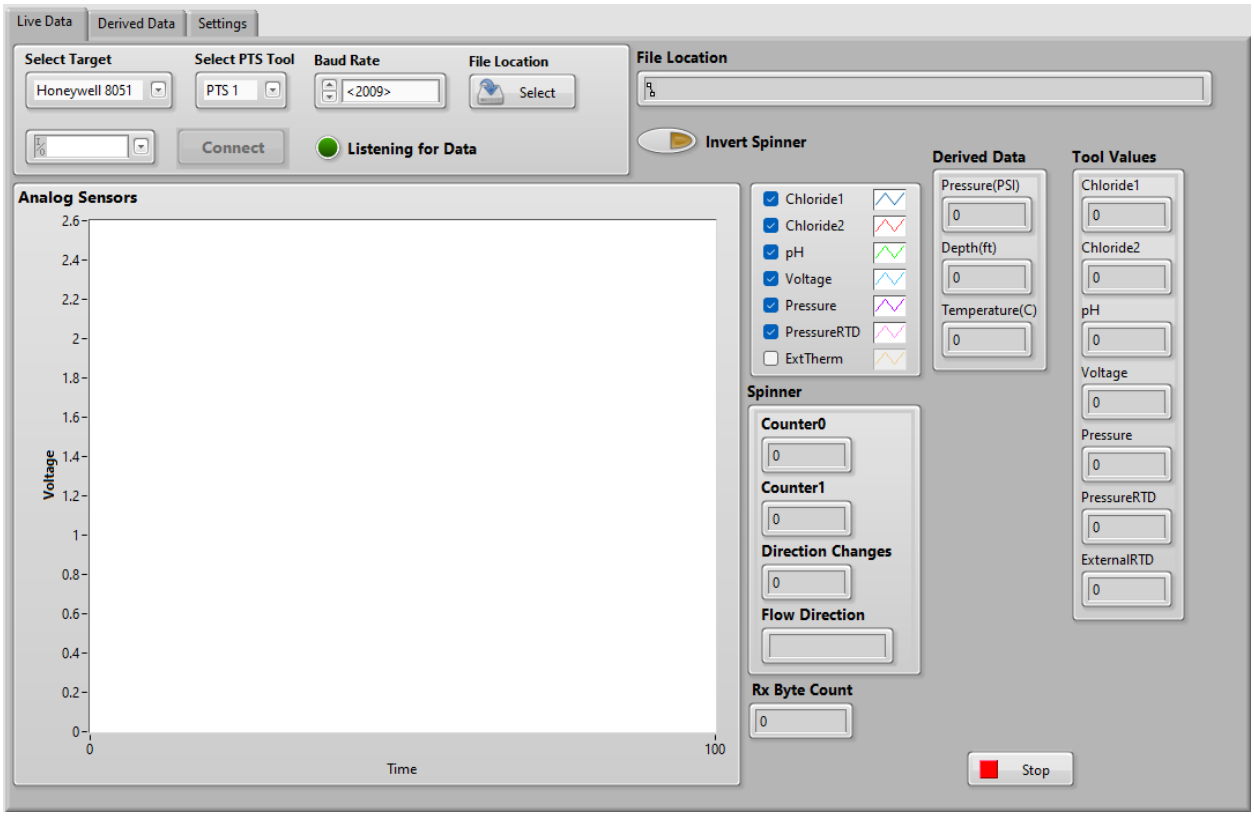

Figure 2-6: LabView User Interface for Field-Scale Chloride Tool

3. Laboratory Experiments

The new iteration of the chloride tool housed two ISE probes, known as ISE probe #2 and ISE probe #3. A calibration was performed to determine an empirical relationship between the voltage readings of the ISE probes and the chloride concentration of the surrounding fluid. The calibration curves for both ISE probes, provided in Equation 3.1 and Equation 3.2, exhibited strong linear relationships ($R^2 = 0.975$ and $R^2 = 0.961$) between their voltage readings and the negative common logarithm of chloride concentration in mol/L.

$$-\log_{10}(\mathrm{M}) = -20.64 * \mathrm{V} + 0.596 \quad \#(3.1)$$
$$-\log_{10}(\mathrm{M}) = -35.31 * \mathrm{V} + 0.550 \quad \#(3.2)$$

Using the calibration curves, the voltage readings from both ISE probes could be converted into chloride concentration values. Flow experiments in the artificial well system in the Stanford Geothermal Laboratory were conducted. The first set of experiments involved the chloride tool being held in a static vertical position in the artificial wellbore while a series of two one-minute feed zone flows occurred. These experiments granted insight into the behavior of the chloride tool in response to varying the parameters needed to infer the feed zone inflow rate in geothermal wells.

The first variables tested were the chloride concentration of the feed zone fluid and the vertical location of the chloride tool relative to the feed zone jet. The results of these experiments are shown in Figure 3-1 and Figure 3-2 for ISE probe #2 and ISE probe #3 respectively.

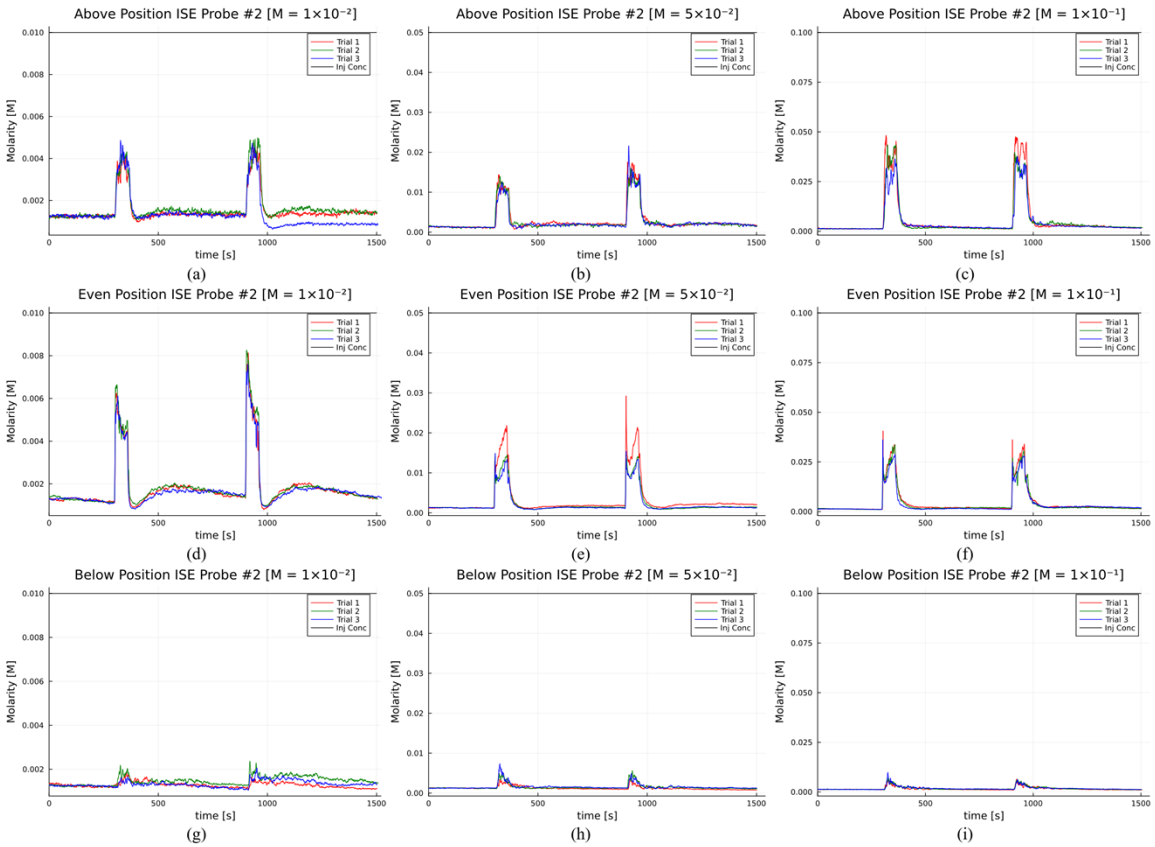

Figure 3-1: Molarity time series for ISE probe #2 in the above, even, and below positions for chloride concentrations of (a, d, and g) 1×10^{-2} mol/L, (b, e, and h) 5×10^{-2} mol/L, and (c, f, and i) 1×10^{-1} mol/L

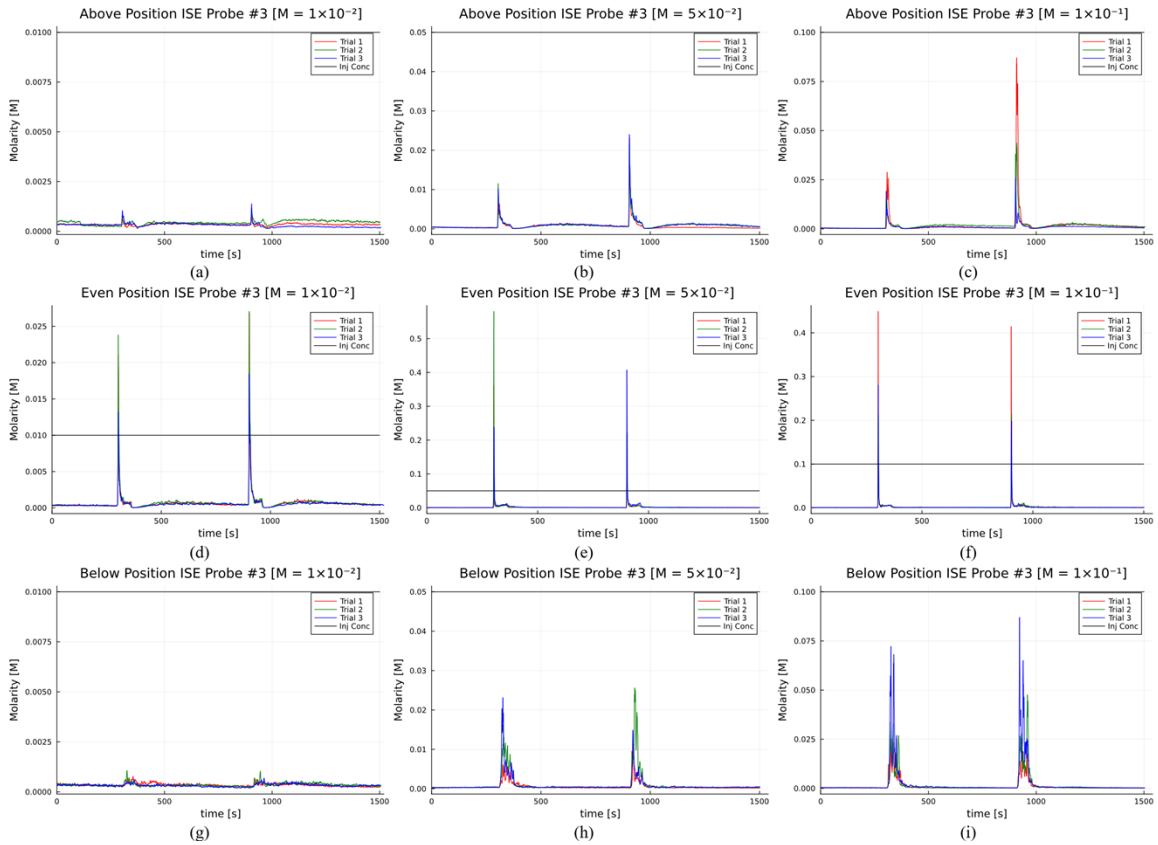

Figure 3-2: Molarity time series for ISE probe #3 in the above, even, and below positions for chloride concentrations of (a, d, and g) 1×10^{-2} mol/L, (b, e, and h) 5×10^{-2} mol/L, and (c, f, and i) 1×10^{-1} mol/L

The most notable result seen in Figure 3-1 and Figure 3-2 was the different behavior of the ISE probes when the chloride concentration of the surrounding fluid changed. Specifically, ISE sensor #2 exhibited smooth and gradual changes to its molarity readings that then plateaued. In contrast, the molarity readings of ISE probe #3 spiked immediately when the chloride concentration of the surrounding fluid changed. Then, the molarity readings of ISE probe #3 decreased, even though no changes to the surrounding fluid occurred. Additionally, these experiments suggested that higher feed zone chloride concentrations produced the most accurate and repeatable responses for both ISE probes.

Additional static experiments with the chloride tool were conducted to determine the effect of varying the feed zone inflow rate and the presence of additional chemical species in the feed zone fluid. The first set of additional experiments found that higher feed zone inflow rates led to higher accuracy when inferring the chloride concentration of the feed zone. The second set of experiments suggested that a significant amount of interference occurred when bromide, and to a lesser extent sulfate, were present in the feed zone fluid. This finding aligns with the literature, which indicates that ion-selective electrodes are imperfectly selective and particularly susceptible to interference from ions such as bromide, iodide, cyanide, silver, and sulfide due to their selectivity coefficients (Baker et al., 1980; Rhodes & Buck, 1980). The interference resulted in the ISE probes massively overestimating the concentration of the individual ions. However, the presence of bromide and

sulfate ions stabilized the readings of the chloride tool when compared to a feed zone fluid containing only bromide, chloride, or sulfate ions. These findings for ISE probe #2 are shown in Figure 3-3.

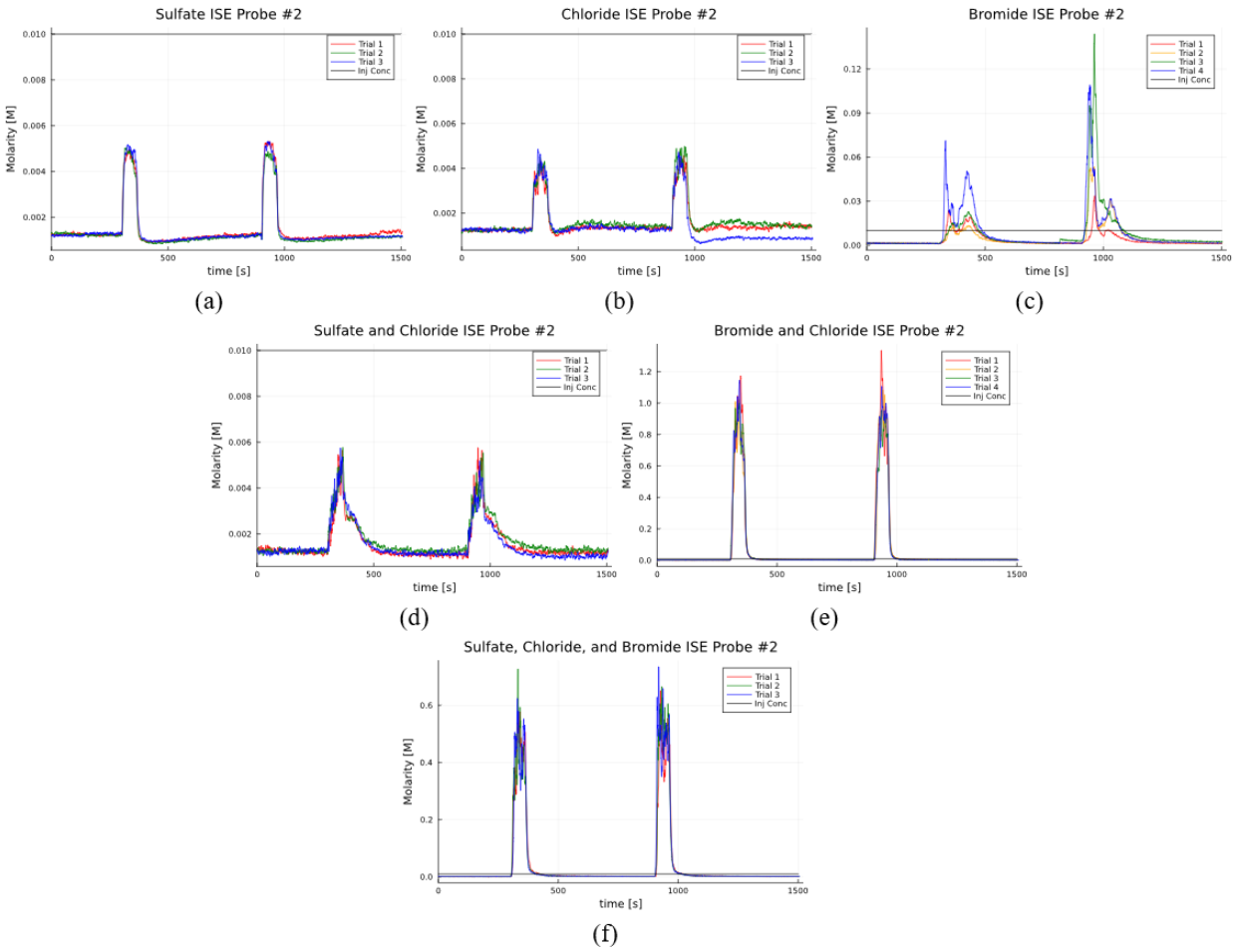

Figure 3-3: Molarity time series for ISE probe #2 for feed zone fluid containing 1×10^{-2} mol/L solutions of (a) sulfate, (b) chloride, (c) bromide, (d) sulfate and chloride, (e) bromide and chloride, and (f) sulfate, chloride, and bromide.

To better imitate field operations, laboratory experiments in which the chloride tool was moved vertically in both directions to measure the chloride concentration across the depth of the artificial wellbore were conducted. These dynamic experiments provided insight into the performance of the chloride tool as it was actuated in the run-in hole (RIH) and pull-out of hole (POOH) directions. The molarity measurements were then used with the analytical solution derived by Sausan et al. (2022) to estimate the mass inflow rate for a single feed zone.

The first series of dynamic experiments tested various chloride concentrations of the feed zone fluid and the direction of motion of the chloride tool. These experiments found that feed zone fluids with higher chloride concentrations resulted in the most accurate feed zone inflow rate inferences. However, these accurate inferences were seen only for ISE probe #3 in the POOH direction. This is likely because the behavior of ISE sensor #3 caused it to best capture the rapid

changes in chloride concentration when the chloride tool moved through the feed zone jet. The results of these experiments are shown in Figure 3-4 and Figure 3-5 for ISE probe #2 and ISE probe #3 respectively. Additionally, Table 3-1 shows the estimates of mass inflow rate $\dot{m}_{in}$ for a single feed zone averaged across the three trials and the percentage error between the actual and inferred inflow rates.

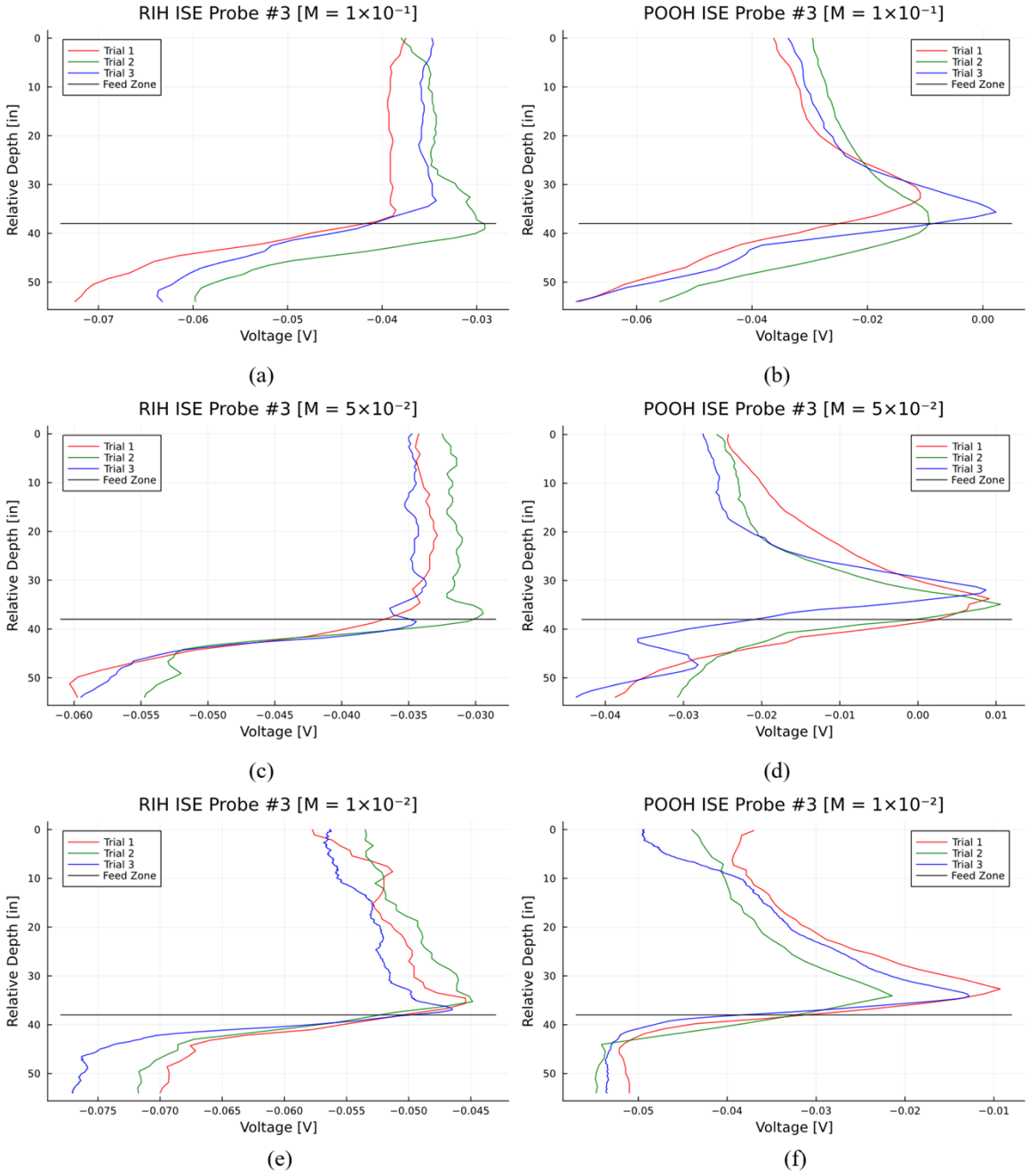

Figure 3-4: Molarity vs. Depth for ISE probe #2 in the RIH and POOH directions for feed zone fluids with chloride concentrations of (a and b) 1×10^{-1} mol/L, (c and d) 5×10^{-2} mol/L, and (e and f) 1×10^{-2} mol/L

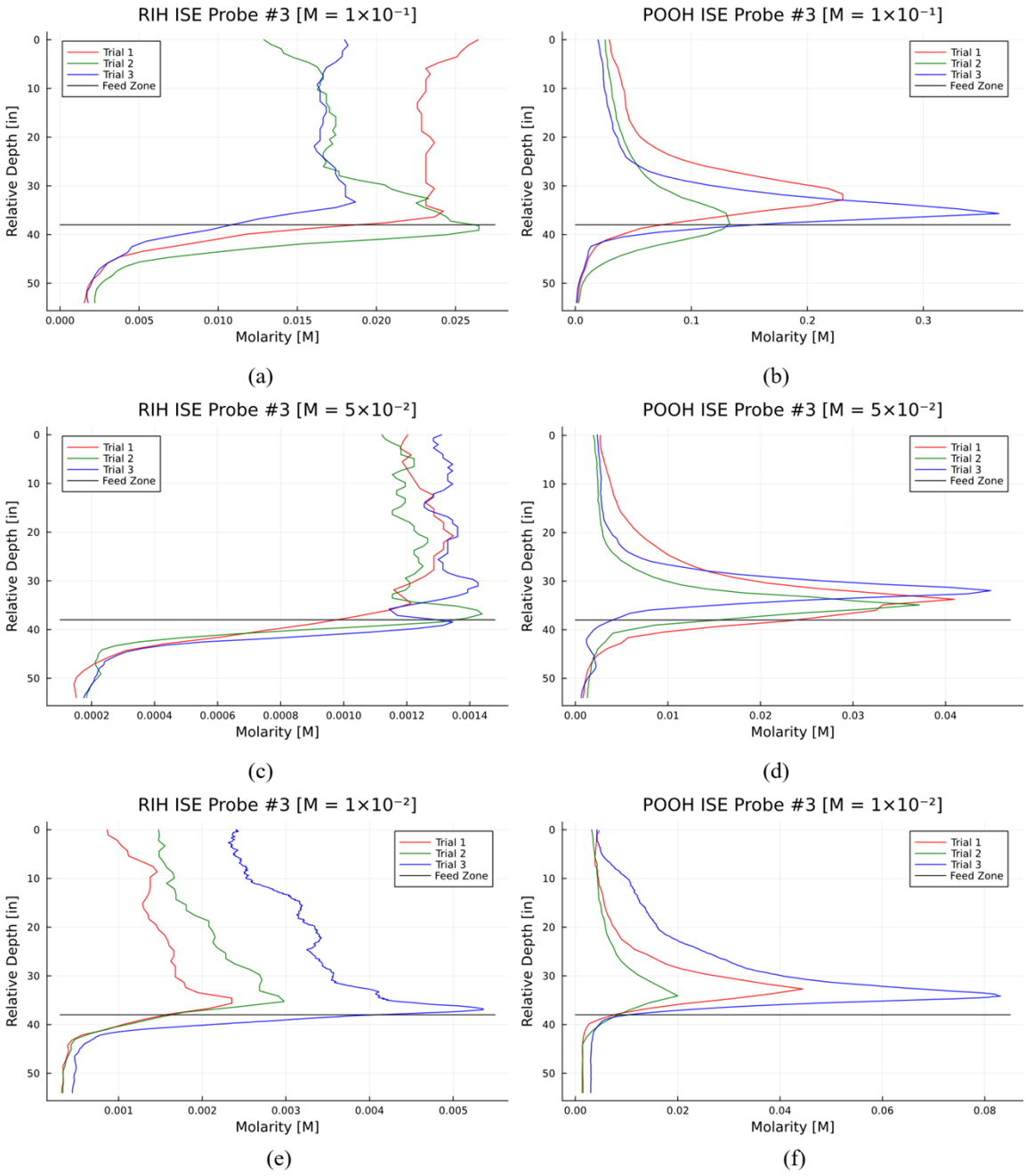

Figure 3-5: Molarity vs. Depth for ISE probe #3 in the RIH and POOH directions for feed zone fluids with chloride concentrations of (a and b) 1×10^{-1} mol/L, (c and d) 5×10^{-2} mol/L, and (e and f) 1×10^{-2} mol/L

Table 3-1: Average inferred feed zone inflow rates and percentage error for the various scenarios at different chloride concentrations of the feed zone fluid

Feed Zone Chloride Concentration	Scenario	ISE Probe	Average Inferred Flow Rate (kg/s)	Percentage Error
1×10^{-1} mol/L	RIH	#2	1.256	993%
1×10^{-1} mol/L	POOH	#2	1.010	778%
1×10^{-1} mol/L	RIH	#3	0.730	535%
1×10^{-1} mol/L	POOH	#3	0.109	-5%
5×10^{-2} mol/L	RIH	#2	1.131	884%
5×10^{-2} mol/L	POOH	#2	0.877	662%
5×10^{-2} mol/L	RIH	#3	0.773	572%
5×10^{-2} mol/L	POOH	#3	0.031	-73%
1×10^{-2} mol/L	RIH	#2	0.866	653%
1×10^{-2} mol/L	POOH	#2	0.886	670%
1×10^{-2} mol/L	RIH	#3	0.393	242%
1×10^{-2} mol/L	POOH	#3	0.078	-33%

Further experiments were conducted to test the following independent variables: the angular position of the chloride tool, the feed zone inflow rate, and the presence of additional ions in the feed zone fluid. These experiments found that the chloride tool underestimated the feed zone inflow rate when the ISE sensors and the feed zone jet were on opposing sides of the well. Additionally, when the feed zone inflow rate was varied, no significant changes to the accuracy of the inferred feed zone inflow rates were seen. Finally, when bromide was present in the feed zone fluid, the magnitudes of the molarity readings were significantly greater than other experiments. However, the relative changes to the measured concentration still provided accurate estimations of the feed zone inflow rate. In contrast, the presence of sulfate ions in the feed zone fluid did not affect the chloride concentration readings of the ISE sensors nor the ability of the chloride tool to infer feed zone inflow rates.

These findings highlight the sensitivity of the chloride tool to multiple parameters that characterize geothermal wells. Overall, these laboratory experiments yielded promising results when measuring a vertical series of chloride concentrations in the artificial geothermal well. As such, the method of inferring feed zone inflow rates in a geothermal well using chloride concentration measurements, albeit on a relative rather than absolute scale, holds promise.

4. Field Testing

The field-deployable chloride tool was deployed in FORGE Wells 58-32, a vertical monitoring well with a total depth of 7,536 ft, and Well 16B(78)-32, a deviated production well drilled to a total depth of 10,947 ft. For 58-32, the weight of the tool was sufficient to lower the tool with gravity; however, in 16B(78)-32, a wireline roller was needed to help convey the tool through the well deviation. Figure 4-1 shows the wells on the Utah FORGE site and Table 4-1 provides an overview of the two FORGE wells and the deployment techniques in each.

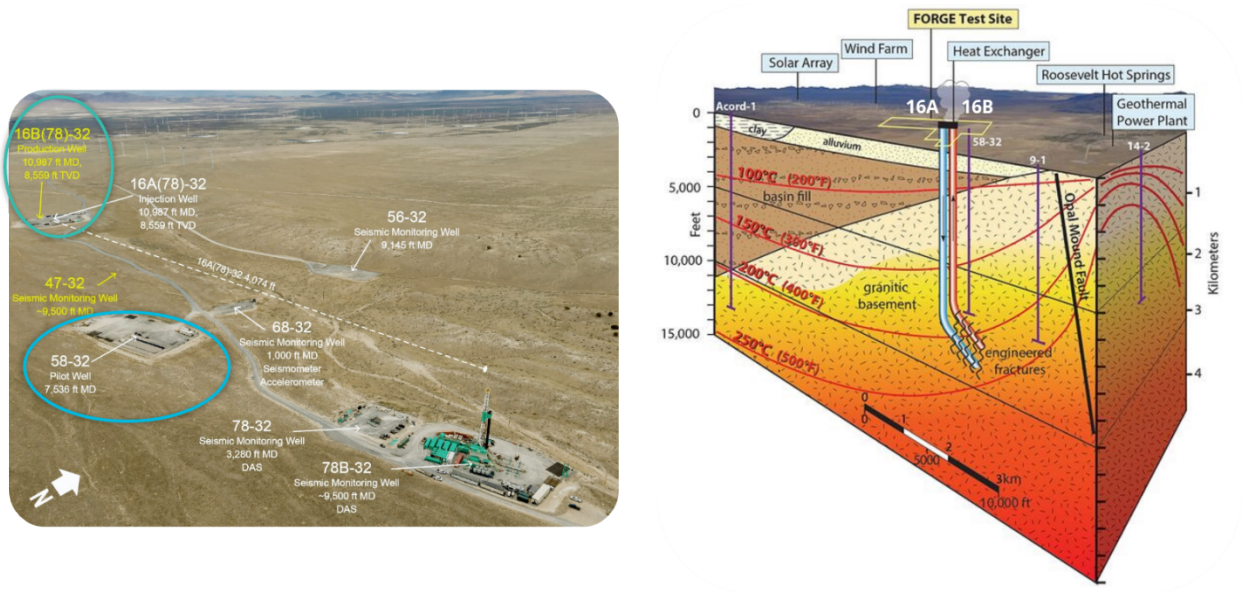

Figure 4.1: Utah FORGE site with planned deployment wells circled (left) and geological and heat model of the Utah FORGE site (right) (source: Utah FORGE)

Table 4-1: Overview of tool deployment scenarios in Utah FORGE wells 58-32 and 16B(78)-32.

FORGE Well	Well Type	Curve Profile	Total Depth	Deployment Technique
58-32	Vertical Pilot Well	N/A	7,536 ft	Tool deployed on Sandia wireline with weight of tool
16B(78)-32	Directional Production Well	5°/100 ft	10,947 ft	Tool deployed through wireline service company with conveyance rollers to assist with well deviation

4.2 FORGE Well 58-32 Deployment

The first deployment was executed June 12-14, 2024, at Utah FORGE Well 58-32, an open and vertical pilot well. Three tool assemblies were prepared for contingency in the field. The Sandia wireline truck was used to deploy the tool into the well and a tip and body centralizer were used to centralize the tool within the 7” casing. The tool was deployed to five test locations shown in Figure 4-2, above, below, and within the cased and perforated zones to test the capability of the ion-selective electrodes to measure chloride concentration readings around the feed zone and determine if these measurements can be used to calculate the feed zone inflow rate.

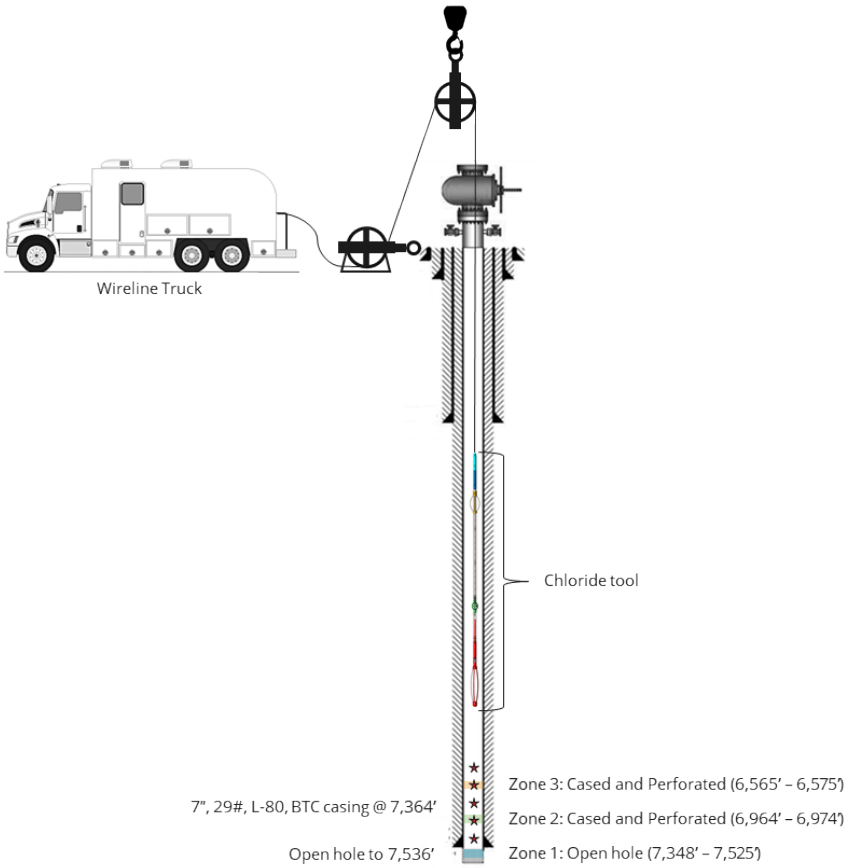

Figure 4-2: Illustration of tool deployment plan for Utah FORGE Well 58-32.

The two primary tools experienced issues during deployment and were pulled out the hole before collecting data. The secondary tool was successfully deployed to 7,168 ft MD with a maximum measured temperature of 190˚C. Measurements were recorded at each test location during the run-in hole (RIH) and pull-out-of-hole (POOH), with noticeably better during the POOH run in comparison to the RIH run. The measurements suggest that there were no internal flows in the well during the logging, which was not unexpected as the well was not producing at the time. Figure 4-3 shows the deployment of the tool into Utah FORGE well 58-32 using the Sandia wireline truck.

Figure 4-3: Deployment at Utah FORGE Well 58-32.

The logging results are shown in Figure 4-4 for the run-in hole (RIH) and Figure 4-5 for the pull-out of the hole (POOH). The first two columns display data from two chemical sensors, while the following two columns show temperature data from the PTS and CPU. The CPU temperature data is considered to be more accurate in magnitude for this particular run, despite the lag in heating up caused by its position inside the electronics component rather than in direct contact with the fluid. The last three columns represent the flow data from the PTS sensor. The perforated zones are marked with yellow regions; the short interval creates the appearance of a line.

A decrease in voltage (i.e., a spike to the left) would correlate with an increase in chloride concentration, indicating inflow presence. If accompanied by a temperature spike coming from geofluid entering the wellbore, the voltage spike will strongly indicate inflow presence. The RIH data shows no strong indication of such a spike around Zone 2 and 3. Meanwhile, spikes in both directions are observed in the chloride voltage columns near Zone 1, which also correlates with a temperature increase. However, the PTS counter did not increase, even with a location pause. Thus, the interval is not interpreted as flowing or experiencing notable internal flow.

The POOH run provides much cleaner data than the RIH run, which was expected as the laboratory experiments have indicated the same behavior. However, chemical sensor voltage data from the shallower part of the POOH, as indicated in Figure 4-5, is erroneous and cannot be used for interpretation. Similar to RIH, spikes are seen near Zone 1 but are not interpreted as flow because

the PTS counter did not change at all. There seems to be a voltage spike near Zone 3, which is also accompanied by a temperature spike. However, the spike was only caused by one data point; again, no corresponding counter or direction change from PTS was present. Thus, it is concluded that the logged interval did not indicate the presence of any inflow. If there were any internal flow happening, it could occur within the open hole section, which was below the maximum depth of our runs as it was considered undesirable to run the tool below the casing shoe.

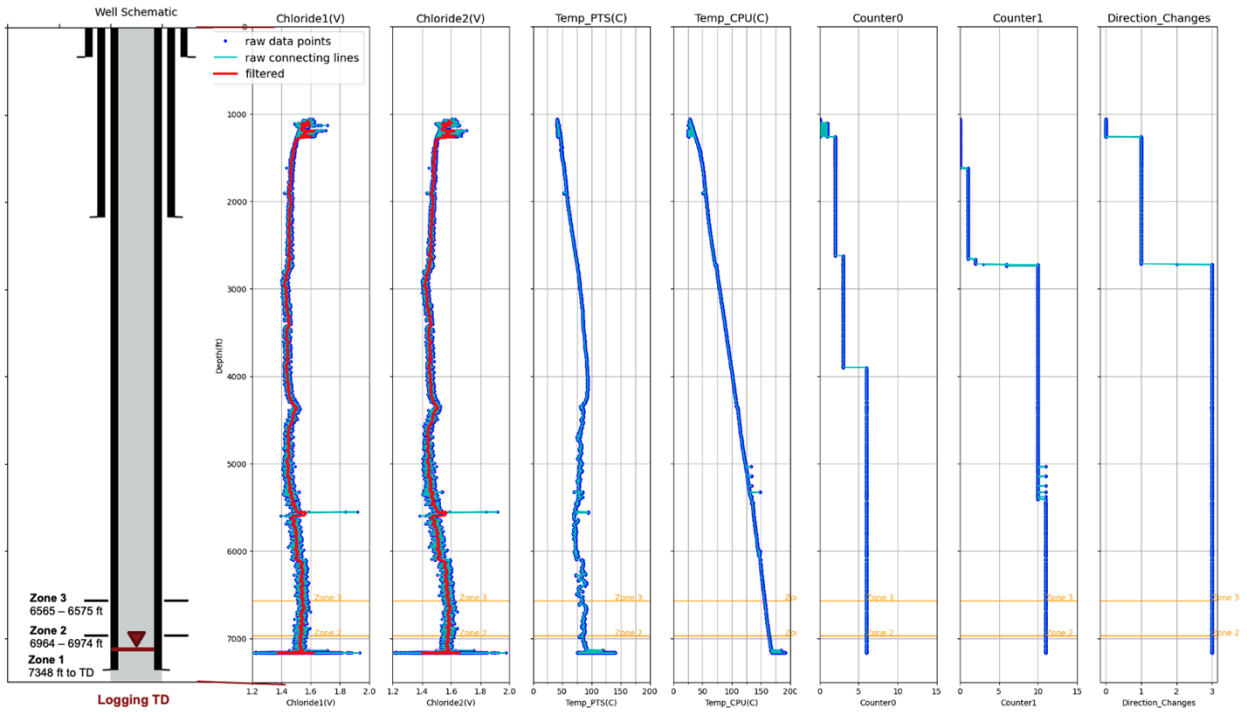

Figure 4-4: logging results during Run in Hole (RIH) at well 58-32.

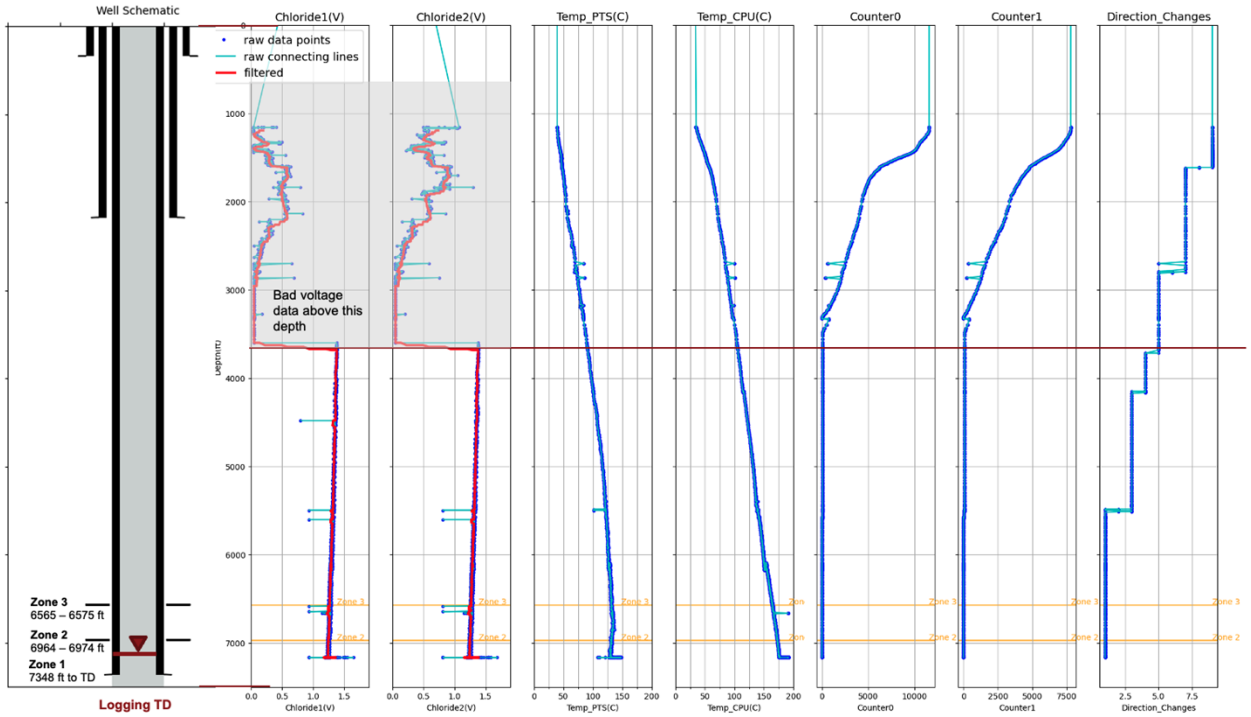

Figure 4-5: logging results during Pull Out of Hole (POOH) at well 58-32.

The voltage signals from the two chemical sensors appear to resemble each other. Thus, the readings from the first sensor were used to evaluate converting the chemical sensor voltage into chloride concentration. Calibration for the field tool used at 58-32 was performed with KCl solution in distilled water and fluid samples from well 16A(78)-32 and 16B(78)-32. The molarity result using the best available calibration curve is shown in Figure 4-6, showing a range of around 0.2 for RIH data and between 0.25 to 0.75 M for POOH data. However, this calibration curve is unreliable due to a discrepancy in the third tool bench calibration after acquisition.

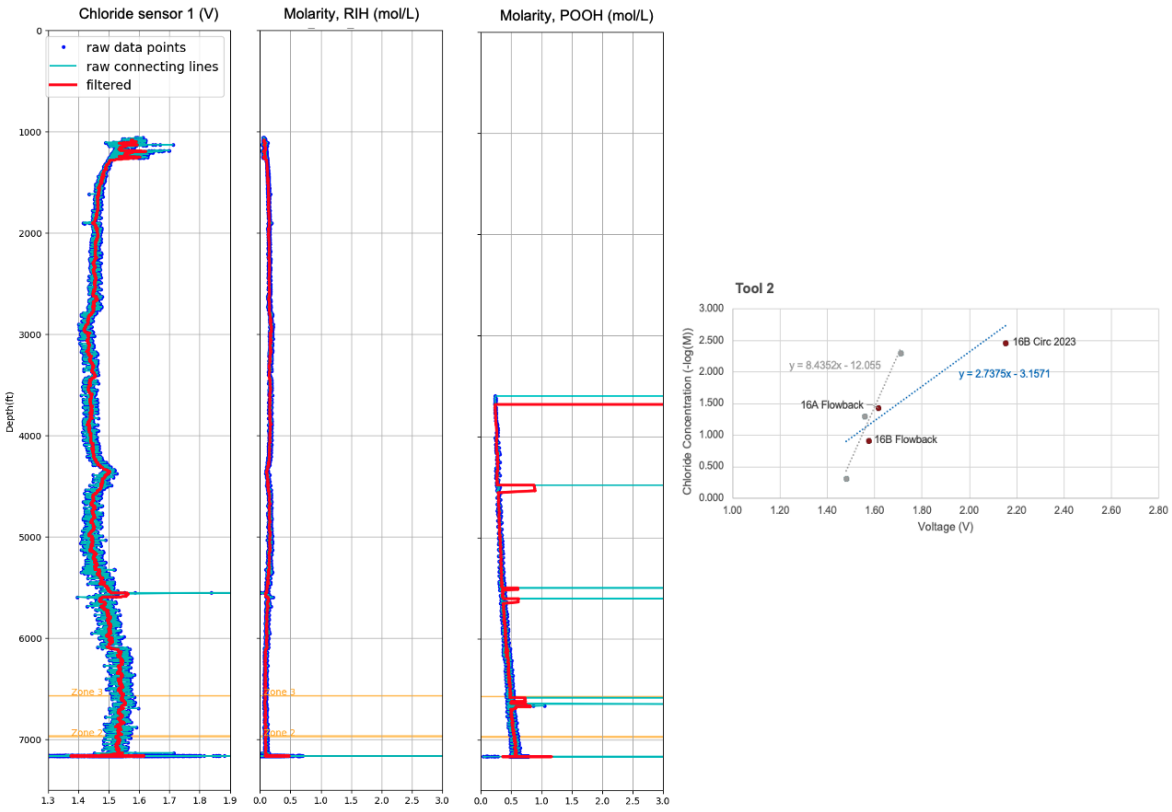

Figure 4-6: converted molarity from the chemical sensor 1 voltage data during RIH and POOH using Tool 2 calibration curve (blue line)

In Table 4-2, the sum of the molarity of relevant chemical species ranges from 0.0046 to 0.12 M. Recent laboratory experiments have shown that in addition to chloride, the ISE is sensitive to bromide (B) and, to a lesser extent, sulfate (SO4), as discussed in Section 3. While chloride is more common in brine water and often determines the molarity, the ISE reacts to bromide and sulfate to varying degrees. The logging results overestimate the chloride concentration compared to available samples, albeit not from well 58-32 itself. Additionally, the RIH data shows a lower concentration than the POOH data, which is closer to the truth. Consequently, improvements will be made to the chemical sensor to ensure more accurate readings for the follow-up test at 16B(78)-32.

Table 4-2; Relevant chemical species of well samples from Utah FORGE Wells 16A(78)-32 and 16B(78)-32

DATE & TIME		WELL	Concentration (mg/l)			Molarity (mol/l)			Sum of molarity (mol/l)
			B	Cl	SO4	B	Cl	SO4	
7/19/2023 20:00		16A(78)-32	2.07	1300	162	2.59E-05	3.66E-02	**1Error! Reference source not found.**.69E-03	0.0383
7/20/2023, 7:50		16B(78)-32	9.05	4384	239	1.13E-04	1.23E-01	2.49E-03	0.1261

7/20/2023, 15:00		16B(78)-32	0.32	122	115	4.01E-06	3.44E-03	1.20E-03	0.0046

4.3 FORGE Well 16B Deployment

The second deployment was conducted August 19, 2024, at Utah FORGE Well 16B(78)-32 during a 30-day circulation test. Two chemical tool assemblies were prepared for contingency in the field. The tool was deployed using an SLB wireline truck, weight bars, and Petromac rollers to assist in conveying the tool through the flowing and deviated well. This test was conducted to test the feasibility of the geochemistry-based approach to map fractures and quantify feed zone inflow rates in a flowing well. Well 16B has five stages, each with 3-5 guns, this provided the opportunity to map up to 20 fractures. For this deployment, ten test locations were planned, to target measurement at and between perforations. For each test location, the tool was held to allow for a stationary measurement of the chloride sensors and PTS tool. The logging between each test location would provide a blind “fly by” measurement to determine the feasibility of mapping fractures using a running log. Figure 4-7 illustrates the deployment plan, with the measurement locations shown as stars and Table 4-3 summarizes the measured depth of the perforation stages and planned and executed test locations during the RIH and POOH logs.

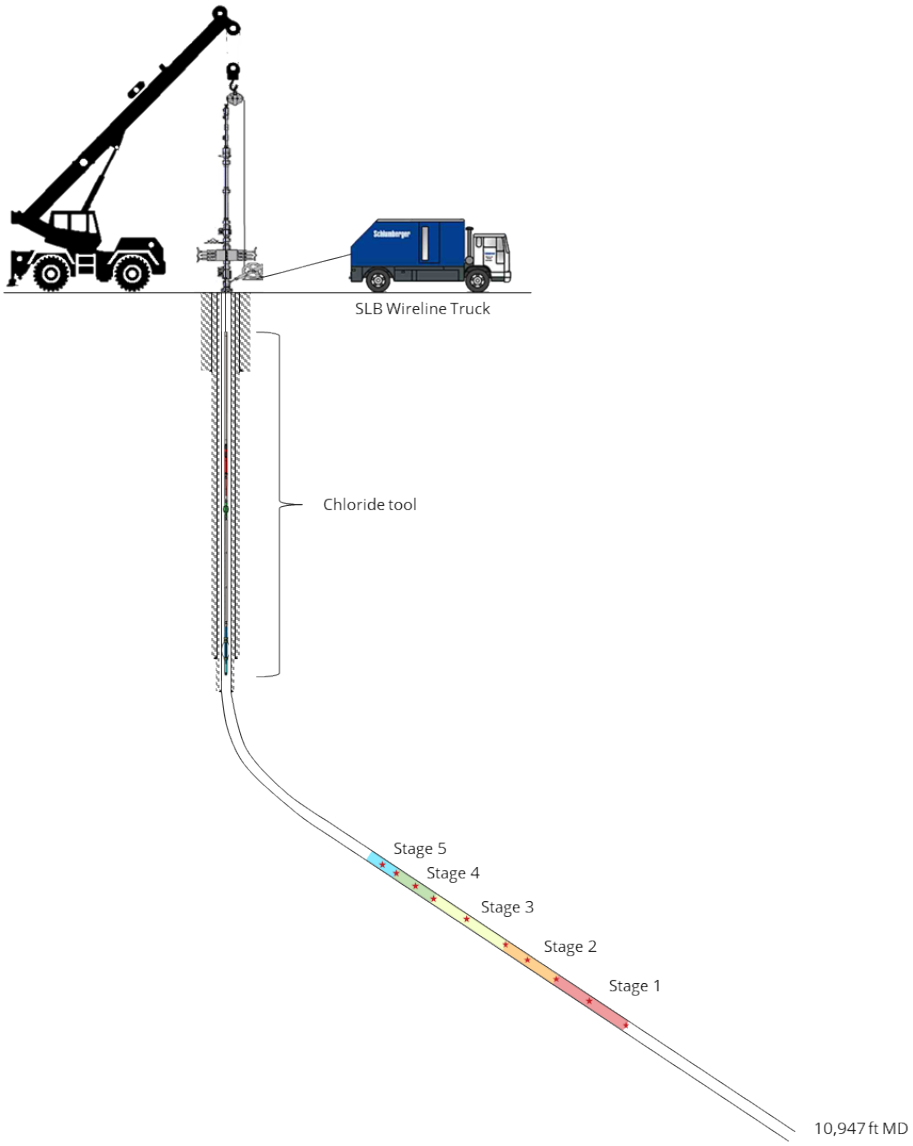

Figure 4-7: Illustration of tool deployment plan for Utah FORGE Well 16B(78)-32. Perforation stages shown in highlighted zones and planned test locations shown as red stars.

Table 4-3: Measured Depth of perforation stages and planned and actual test locations.

	Measured Depth (ft)							
	Gun 1	**Gun 2**	**Gun 3**	**Gun 4**	**Gun 5**	**Planned Test Location**	**Actual RIH Test Location**	**Actual POOH Test Location**
Stage 5	8500 - 8806	8806 - 8855	8855 - 8876	8876- 8920		8865	8865	8865
						8920	8920	8920
Stage 4	8920 - 8978	8978 - 9013	9013 - 9042	9042 - 9155		9030	9030	9030
						9155	9155	9155
Stage 3	9155 - 9306	9306 - 9368	9368 - 9407			9388	9388	9388
						9407	-	-
Stage 2	9407 - 9440	9440 - 9455	9455 - 9469	9469 - 9495	9495 - 9600	9462	-	-
						9600	-	-
Stage 1	9600 - 9720	9720 - 9753	9753 - 9765	9765 - 9800		9759	-	-
						9800	-	-

The tool was successfully deployed to approximately 9,480 ft with a maximum measured temperature on the tool of 210°C. Figure 4-8 shows the fully assembled tool being loaded into the lubricator by the SLB team and Figure 4-9 shows the Utah FORGE Well 16B test site during the logging. The monitor wellhead pressure, flowline temperature, and separator liquid discharge flow during the log were 260-263 psi, 180°C, and 294-330 gpm, respectively. Measurements were recorded through Stage 3, at which point the log began to show potential issues. The wireline operator noted the tool had stopped moving at approximately 9,480 ft. After recovering tension in the line, the tool was brought back up the well for the POOH log to record measurements in Stage 4 and 5. The measurements in the RIH log were of noticeably better quality than the POOH log, potentially indicating damage to the tool. The measurement results indicate a change in chloride concentration in the perforation zones, suggesting the chemical tool is capable of mapping fractures in a flowing well.

Figure 4-8: Full chemical tool assembly attached to weight bars and being loaded into lubricators.

Figure 4-9: Utah FORGE Well 16B test site with lubricator stacks for chemical tool.

5. Conclusion

The latest updates on the chloride tool development have focused on the deployment of the field-scale tool at the Utah FORGE site. Three assembled field-scale tools were constructed and tested in the lab, testing different iterations of the sensor pellet, tool housing, data electronics package, and assembly, and confirming operation of the tool on the wireline. The tool assembly features a Mitco PTS sensor package for secondary measurements, a wire guide component, chemical sensor housing, and HTHP electronics for data transmission through a 7-conductor feedthrough to the wireline. The sensor housing was fabricated using metal additive manufacturing, and was designed to integrate with the logging tool, accommodating Ion-selective Electrode (ISE) sensors, reference sensors, and pH sensors to be exposed to the flow in the well.

Concurrent with the development of the field-scale tool, flow experiments were conducted in the artificial well system at the Stanford Geothermal Lab. These laboratory experiments provided insights into the chemical tool's response to varying parameters, including chloride concentration in the feed zone, the tool's vertical position relative to the feed zone, and the presence of additional chemical species in the feed zone fluid. The findings demonstrated the chemical tool's sensitivity to multiple parameters, suggesting that using chloride concentration measurements to infer feed zone inflow rates in geothermal wells is a promising method.

The tool was successfully deployed at FORGE Well 58-32 an open, vertical well in June 2024, and FORGE Well 16B(78)-32, a pressurized and flowing deviated well in August 2024. Both deployments demonstrated the capability of the tool to withstand Utah FORGE conditions, and the feasibility of a geochemistry-based approach to map fractures in a flowing well (16B), with no false positives in a nonflowing well (58-32).

ACKNOWLEDGMENTS

This work is part of the Utah FORGE project under award number 3-2418 as a collaborative project between Stanford University and Sandia National Laboratory, supported by the U.S. Department of Energy. Sandia National Laboratories is a multimission laboratory managed and operated by National Technology & Engineering Solutions of Sandia, LLC, a wholly owned subsidiary of Honeywell International Inc., for the U.S. Department of Energy’s National Nuclear Security Administration under contract DE-NA0003525. This paper describes objective technical results and analysis. Any subjective views or opinions that might be expressed in the paper do not necessarily represent the views of the U.S. Department of Energy or the United States Government. Paper registration ID: SAND2024-11132C.

The authors would also like to extend their gratitude to SLB and the Utah FORGE team for their invaluable support in the field deployment effort.

REFERENCES

Acuña, J. A. and. Arcedera B. A.: Two-Phase Flow Behavior and Spinner Data Analysis in Geothermal Wells, Proceedings 13th Workshop on Geothermal Reservoir Engineering, Stanford University, Stanford, California (2005).

Baker, C. Kahn, S.E., Bermes, E.W.: Effect of Bromide and Iodide on Chloride Methodologies in Plasma or Serum. Annals of Clinical and Laboratory Science, Vol. 10, No. 6 (1980).

Chen, Y.; Selvadurai, A. P. S.; Zhao, Z. Modeling of Flow Characteristics in 3D Rough Rock Fracture with Geometry Changes under Confining Stresses. Computers and Geotechnics 130, 103910 (2021).

Co, C..,Pollard, D., Horne, R. Towards a Better Understanding of the Impact of Fracture Roughness on Permeability-Stress Relationships Using First Principles. Proceedings 42nd Workshop on Geothermal Reservoir Engineering, Stanford University, Stanford, California (2017).

Fei, F., Lu, Y., Bunger, A. P., & Cusini, M.: Experimental and Numerical Study of Hydraulic Fracturing in Enhanced Geothermal Systems (EGS), Proceedings 48th Workshop on Geothermal Reservoir Engineering, Stanford University, Stanford, California (2023).

Fu, P., Schoenball, M., Morris, J., Ajo-Franklin, J., Knox, H., Kneafsey, T., Burghardt, J., White, M.: Microseismic Signatures of Hydraulic Fracturing: A Preliminary Interpretation of Intermediate-Scale Data from the EGS Collab Experiment. Proceedings 44th Workshop on Geothermal Reservoir Engineering, Stanford University, Stanford, California (2019).

Gao, X., Egan, S., Corbin, W.C., Hess, R.F., Cieslewski, G., Cashion, A.T., and Horne, R.N.: Analytical and Experimental Study of Measuring Enthalpy in Geothermal Reservoirs with a Downhole Tool, GRC Transactions, Vol.41(2017).

Hess, R., Boyle, T., Limmer, S., Yelton, W., Bingham, S., Stillman, G., Cieslewski, G.: Real-Time Downhole Measurement of Ionic Tracer Concentration and pH in Geothermal Reservoirs, GRC Transactions, Vol. 38 (2014).

Huenges, E.: 25 - Enhanced geothermal systems: Review and status of research and development, Geothermal Power Generation, Woodhead Publishing, Pages 743-761, (2016).

Ishibashi, T., Watanabe, N., Hirano, N., Okamoto, A., and Tsuchiya, N.: Upgrading of Aperture Model based on Surface Geometry of Natural Fracture for Evaluating Channeling Flow, GRC Transactions, 36, (2012), 481-486.

Judawisastra, L. H., Sausan, S., Cherng-Su, J., Horne, R. N.: Development Update on Chloride-based Inflow Measurement in Fractured Enhanced Geothermal Systems (EGS) Wells, Proceedings 48th Workshop on Geothermal Reservoir Engineering, Stanford University, Stanford, California (2023).

Judawisastra, L. H., Sausan, S., Horne, R. N.: Analytical, Experimental and Numerical Development Update on Inflow Measurement in Geothermal Wells from Chloride Concentration. Proceedings, 8th Indonesia International Geothermal Convention & Exhibition, (2022).

Rhodes, R. K., Buck, R. P.: Competitive Ion-Exchange Evaluation of the Bromide Interference on Anodized Silver/Silver Chloride Electrodes, Analytica Chimica Acta, Volume 113, Issue 1, (1980).

Sausan, S., Judawisastra, L. H., Horne, R. N.: Development of Downhole Measurement to Detect Inflow in Fractured Enhanced Geothermal Systems (EGS) Wells, Proceedings 47th Workshop on Geothermal Reservoir Engineering, Stanford University, Stanford, California (2022).

Sausan, S., Judawisastra, L. H., Cherng-Su, J., Horne, R. N.: Chloride-based Wireline Tool for Measuring Feed Zone Inflow in Enhanced Geothermal Systems (EGS) Wells: Experimental, Numerical, and Data-driven Updates, Geothermal Resources Committee Transactions Vol 47 (2023), pg. 841-863.

Sausan, S., Hartung M. B., Cherng-Su, J., Schneider, M., Wright, A. A., Horne, R.: Updates on the Development of Chloride-based Wireline Tool for Measuring Feed Zone Inflow in Enhanced Geothermal Systems (EGS) Wells, Proceedings 48th Workshop on Geothermal Reservoir Engineering, Stanford University, Stanford, California (2024).

Sausan, Sarah: Investigating Fluid Flow Behavior in Enhanced Geothermal System (EGS) Wells: Numerical and Data-Driven Approaches, MS Thesis, Energy Resources Engineering Department, Stanford University (2023).

Sisler, J., Zarrouk, S. J., Adams, R.: Improving the Performance of Geothermal Pressure, Temperature and Spinner (PTS) Tools Used in Down-Hole Measurements. Proceedings, World Geothermal Congress 2015, Melbourne, Australia (2015).

Sullivan, J.L., Clark, C.E., Han, J., Wang, M.: Life-Cycle Analysis Results of Geothermal Systems in Comparison to Other Power Systems, Argonne National Laboratory ANL/ESD/10-5 (2010)

Xiao, F., Shang, J., Wanniarachchi, A., Zhao, Z.: Assessing Fluid Flow in Rough Rock Fractures Based on Machine Learning and Electrical Circuit Model. Journal of Petroleum Science and Engineering, 206, 109126 (2021).

Zhang, Y., Chai, J.: Effect of Surface Morphology on Fluid Flow in Rough Fractures: A Review. Journal of Natural Gas Science and Engineering 79, 103343 (2020).